Effect of particles on hydrodynamics and mass transfer in a slurry bubble column: Correlation of experimental data

Huahai Zhang[1], Zhongshan Guo[1,2], Yuelin Wang[1], Xiankun Shen[1], Tiefeng Wang[1]*

1. Beijing Key Laboratory of Green Reaction Engineering and Technology

Department of Chemical Engineering, Tsinghua University, Beijing 100084, China

2. Ningmei Coal to Oil Branch Company, CHN Energy, Yinchuan 750411, China

Correspondence author: Tiefeng Wang (E-mail: wangtf@tsinghua.edu.cn)

Abstract:

The effects of particle concentration and size on hydrodynamics and mass transport in a slurry bubble column were experimentally studied. With increasing particle concentration, the averaged gas holdup, gas holdup of small bubbles and gas-liquid volumetric mass transfer coefficient decreased, while the gas holdup of large bubbles increased slightly. With increasing particle size, the averaged gas holdup and $k_l a$ remained unchanged when the particle size increased from 55 to 92 μm, but decreased significantly when the particle size was further increased to 206 μm. A liquid turbulence attenuation model which could quantitatively describe the effects of particle concentration and size was first proposed. Semi-empirical correlations were obtained based on extensive experimental data in a wide range of operating conditions and corrected liquid properties. The gas holdup and mass transfer coefficient calculated by the correlations agreed with the experimental data from both two-phase and three-phase bubble columns.

Key words: Slurry bubble column, Particle concentration, Particle size, Liquid turbulence attenuation, Semi-empirical correlations

1. Introduction

Slurry bubble column reactors are widely used in petrochemical and mineral processing and wastewater treatment processes, because of their advantages, namely, simple geometry, better temperature control and heat removal, high mass transfer rates, low operation and maintenance costs, and higher durability of catalyst.[1,2] However, their complicated hydrodynamics and mass transfer behaviors make them difficult to design and scale up,[3,4] where, in addition, solid catalyst particles have complex effects on their hydrodynamics and mass transfer rates.[5-8] Therefore, it is necessary to understand the effects of solid particle concentration and size for the operation and scale up of these reactors.

Extensive experiments have shown that particle concentration and size have complicated effects on the gas holdup,[5,9] bubble size,[10,11] and mass transport.[8,12] Generally, with increasing particle concentration, the bubbles becomes larger,[9-11,13] which leads to lower gas holdup α_g[9,14] and volumetric gas-liquid mass transfer coefficient $k_l a$.[12,15-17] Nevertheless, there is no reported general trend for the effect of particle size on the hydrodynamics and mass transport. Ojima et al.[18,19] found that the local gas holdup and bubble frequency increased with particle size from 60 to 150 μm. Using micron-sized hydrophilic glass beads particles of 11, 35 and 93 μm, Li et al.[20] also found that the total gas holdup and small bubble gas holdup increased with increasing particle size, while the rising velocity of large bubbles decreased with particle size. However, an increase in averaged bubble size and a decrease in averaged gas holdup with increasing particle size were reported by Rabha et al.[10] and Lakhdissi

et al.[5] Meanwhile, Lakhdissi et al.[8] further reported that solid particles have a negligible effect on k_la in experiments using two particles sizes (71 and 156 μm) and three volume concentrations (1%, 3%, 5%). However, data with higher concentrations of particles and wider particle size ranges on k_la are very sparse at present.

On the other hand, the mechanisms of the particle effects on the hydrodynamics and mass transfer behavior have not been comprehensively studied. Fig. 1 summarizes the following four recognized particle effects in a slurry bubble column:

(1) Increased apparent slurry viscosity.[1] Many empirical correlations[21-25] for the apparent liquid viscosity due to the addition of solid particles were reported, which showed that the apparent viscosity increased with increasing particle concentration.

(2) Enhanced bubble coalescence. Ojima et al.[18,19] quantitatively investigated the effect of particle concentration (0 – 50 vol/vol%) and particle size (60, 100, and 150 μm) on the film drainage time in quasi two-dimensional slurry bubble flow using high-speed camera. They found that with increasing particle concentration or decreasing particle size, the liquid film drainage time decreased, leading to enhanced bubble coalescence.

(3) Reduced drag force.[26] Wang et al.[27] studied the rising of bubbles coated to varying degrees by glass-bead particle, and found that with the addition of particles, the bubbles became more spherical. Due to the decrease of pressure drag and friction drag as compared to irregularly shaped bubbles, the drag force on the coated spherical bubbles was reduced.

(4) Attenuated liquid turbulence.[28-30] Li and Zhong[31] used an Eulerian-Eulerian-

Eulerian three-fluid approach to simulate a gas-liquid-solid three-phase bubble column, and found that the instantaneous liquid turbulent dissipation rate and turbulent kinetic energy decreased rapidly with increasing particle concentration. Using the direct numerical simulation of particle-laden isotropic turbulence, Squires and Eaton[29] also saw an attenuating effect due to particles.

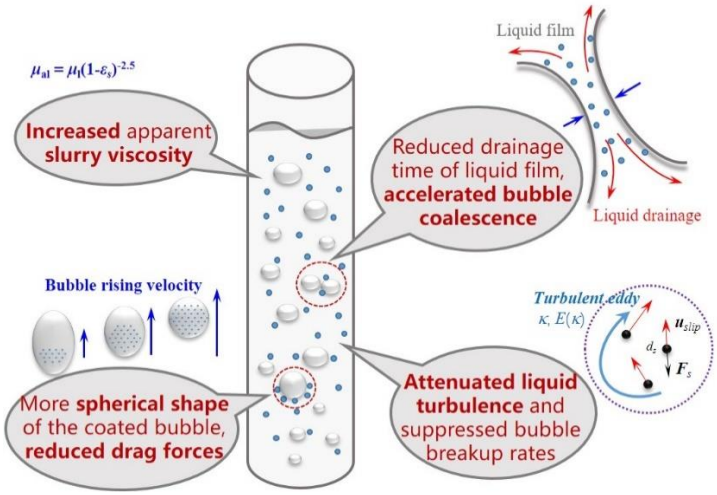

Figure 1. Schematic of the mechanisms of the effect of particle.

Gas holdup and k_la in a slurry bubble column are usually calculated by considering the liquid and solid phases as a slurry or pseudo-homogeneous phase.[32-34] Thus, in these works, only the slurry physical properties such as density and viscosity were changed, and the two-phase model was used to work with a three-phase system. However, this approach fails to capture the effect of enhanced bubble coalescence, reduced drag force and attenuated liquid turbulence.

This work studies the effect of particles in a wide range of particle volume concentration (0 – 20%) and particle size (55 – 206 μm) on hydrodynamics and mass transport in a slurry bubble column. Empirical correlations for the gas holdup and k_la

in a gas-liquid bubble column were developed using regression to our experimental data and typical results in the literature. A theoretical model of dominant liquid turbulence attenuation was also developed based on equalizing the energy consumed by the relative motion of the particles and the attenuated liquid turbulence energy calculated from the turbulent energy spectrum. After analyzing the above mechanisms of the particle effects, the empirical correlations we developed for gas-liquid system were extended to a gas-liquid-solid three-phase system. Calculated gas holdup and $k_l a$ from these empirical correlations were in good agreement with experimental data, in both gas-liquid and gas-liquid-solid bubble columns.

2. Experimental

2.1 Experimental setup

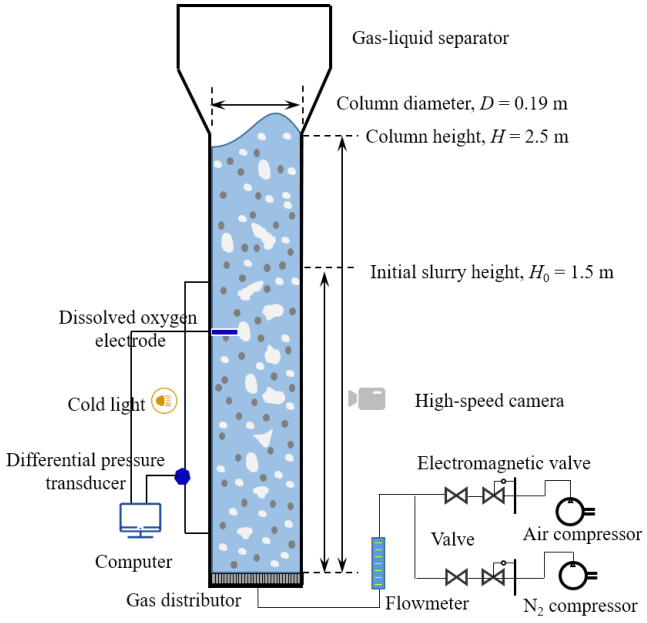

Figure 2. Schematic of the experimental set-up.

A Plexiglas slurry bubble column with diameter D_c = 0.19 m and height H = 2.5 m, as shown in Fig. 2, was used in this work. The gas distributor was a perforated plate

with an orifice diameter of 1 mm and a triangular pitch distance of 9 mm. Air was used as the gas phase, deionized water (ρ_l = 1000 kg/m^3, σ_l = 72.5 mN/m, μ_l = 1 mPa·s) was used as the liquid phase, and hydrophilic glass bead (ρ_s = 2400 kg/m^3, d_s = 55, 92, and 206 μm, α_s = 0 – 20 %) was used as the solid phase.

2.2 Measurement techniques and methods

Two differential pressure transducers installed at 0.03 and 1.4 m above the gas distributor were used to record the pressures. The average gas holdup was measured from the pressure drops Δp and calculated by:

$$\alpha_g = 1 - \frac{1}{\rho_l + \alpha_s(\rho_s - \rho_l)} \cdot \frac{\Delta P}{g\Delta h} \tag{1}$$

A quick cut-off electromagnetic valve was installed in the gas inlet pipe for the dynamic gas disengagement (DGD) experiments. DGD experiments were performed to investigate the gas phase structure. In the DGD experiments, the gas supply was quickly shut-off and the gas holdup variation with time was monitored. Typical DGD curves for the effect of particle concentrations on gas holdup are shown in Fig. 3. Since large bubbles rise faster than small bubbles, the gas holdup variation with time has two different stages: it decreased fast in the first stage, and decreased gradually in the second stage.[35] Fig. 3 shows that with increasing particle concentration α_s, the averaged gas holdup and gas holdup of small bubbles significantly decreased.

The gas-liquid volumetric mass transfer coefficient k_la was measured using the oxygen desorption method using a switch from N_2 to air. An optical probe was used to measure the dissolved oxygen concentration $C_{O_2}(t)$ in liquid water at 1.0 m above the gas distributor. Typical curves of dissolved oxygen concentration versus time with U_g

as parameter are shown in Fig. 4. The value of $k_l a$ was determined by the following equations, which are based on a CSTR model:[36]

$$\frac{dC_{O_2}(t)}{dt} = k_l a\left[C^*_{O_2} - C_{O_2}(t)\right] \tag{2}$$

$$\int_{C_{O_2}(t=0)}^{C_{O_2}(t)} -\frac{1}{C_{O_2}(t) - C^*_{O_2}} dC_{O_2}(t) = k_l a t \tag{3}$$

$$\ln\left[\frac{C^*_{O_2} - C_{O_2}(t)}{C^*_{O_2} - C_{O_2}(t=0)}\right] = k_l a t \tag{4}$$

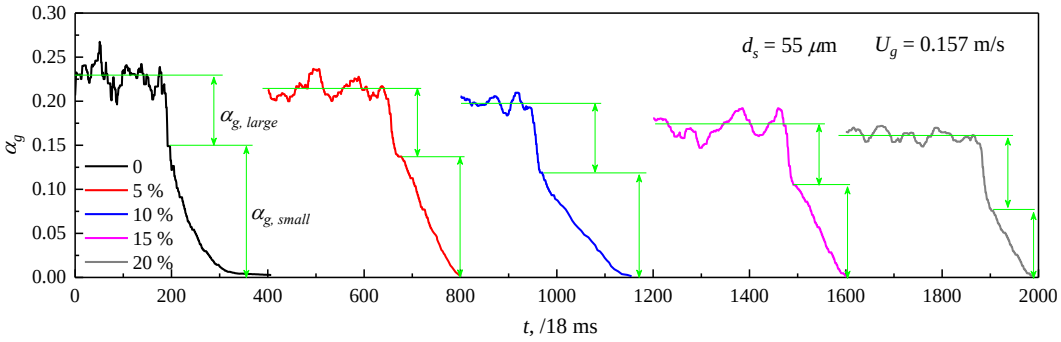

Figure 3. Typical dynamic gas-disengagement profiles at U_g = 0.157 m/s and different particle concentrations.

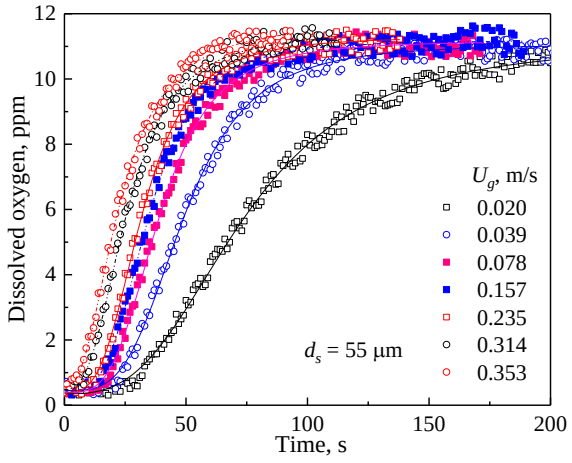

Figure 4. Typical DO profiles during the "gassing on" period at different superficial gas velocity (5% glass beads).

2.3 Results and discussion

2.3.1 Effect of particle concentration

Gas holdups

Fig. 5 shows the effect of superficial gas velocity on the averaged gas holdup α_g, gas holdup of small bubbles $\alpha_{g,small}$ and large bubbles $\alpha_{g,large}$ at different particle concentrations α_s. At each α_s, the influence of U_g on α_g, $\alpha_{g,small}$ and $\alpha_{g,large}$ followed the same trend. The value of $\alpha_{g,small}$ increased significantly with U_g in the homogeneous regime, while it remained unchanged in the heterogeneous regime. In contrast, $\alpha_{g,large}$ is linearly proportional to U_g due to the enhanced bubble coalescence.

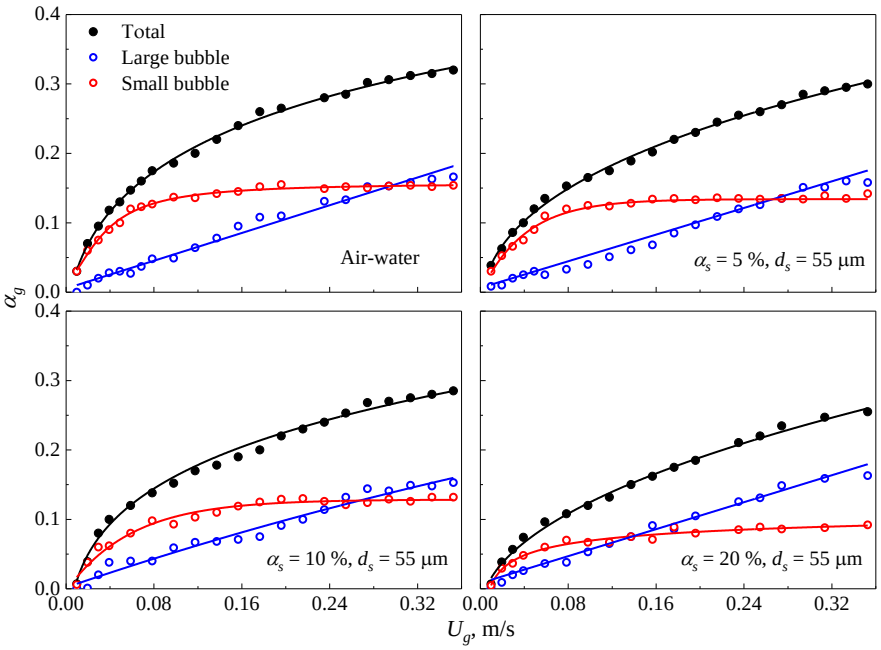

Figure 5. Effect of particle concentration on total gas holdup, and gas holdup of large bubbles and small bubbles.

By comparing the gas holdup at different α_s, it is seen that α_g and $\alpha_{g,small}$ significantly decreased with increasing α_s, while $\alpha_{g,large}$ slightly increased. Li et al.[14] reported similar results of the effect of α_s on α_g and $\alpha_{g,small}$, but they found that $\alpha_{g,large}$

slightly decreased when increasing α_s from 0 to 40%. Many researchers[11,26] ascribed the decrease in α_g to increased apparent liquid viscosity and enhanced bubble coalescence. However, with an increase of α_s from 0 to 20%, the apparent liquid viscosity only increased 2-3 times.[22,23,25] Lakhdissi et al.[5], An et al.[28] and Xing et al.[35] demonstrated that this slight increase in viscosity could not explain the significant variation of gas holdup. In addition, An et al.[28] found by CFD simulation that enhanced bubble coalescence was also not enough to cause a large difference in α_g, and they proposed that turbulence attenuation plays the most important role. We discuss this in Section 3.3.

Volumetric mass transfer coefficient

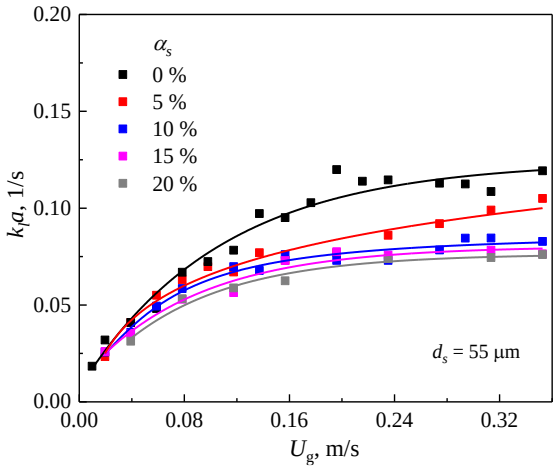

Figure 6. Effect of particle concentration on the volumetric mass transfer coefficients.

Fig. 6 shows the effect of particle concentration on $k_l a$. With increasing α_s, $k_l a$ significantly decreased due to decreased gas holdup and a larger bubble size range, which was previously reported by many researchers.[12,15-17] However, Lakhdissi et al.[8] reported that at $\alpha_s \leq 5\%$ the particles had a negligible effect on $k_l a$ due to two opposite effects, namely the gas-liquid interfacial area decreased while the liquid-side mass

transfer coefficient increased with the addition of particles.

2.3.2 Effect of particle size

Gas holdup

The effects of particle size on the averaged gas holdup at different α_s are shown in Fig. 7. The averaged gas holdup at d_s = 55 and 92 μm were almost the same. In contrast, there was an obvious decrease in α_g when particle size increased to 206 μm. Although Ojima et al.[19] reported that the particle size affects bubble coalescence, An et al.[28] demonstrated that this effect could not explain the decreased gas holdup. Recently, Lakhdissi et al.[5] found that particles collided with the bubbles in a slurry bubble column, which decreased the bubble rise velocity, and accordingly proposed a hindering factor to account for this. By considering the hindering factor, the effects of particle size and concentration on the gas holdup were well described.[5]

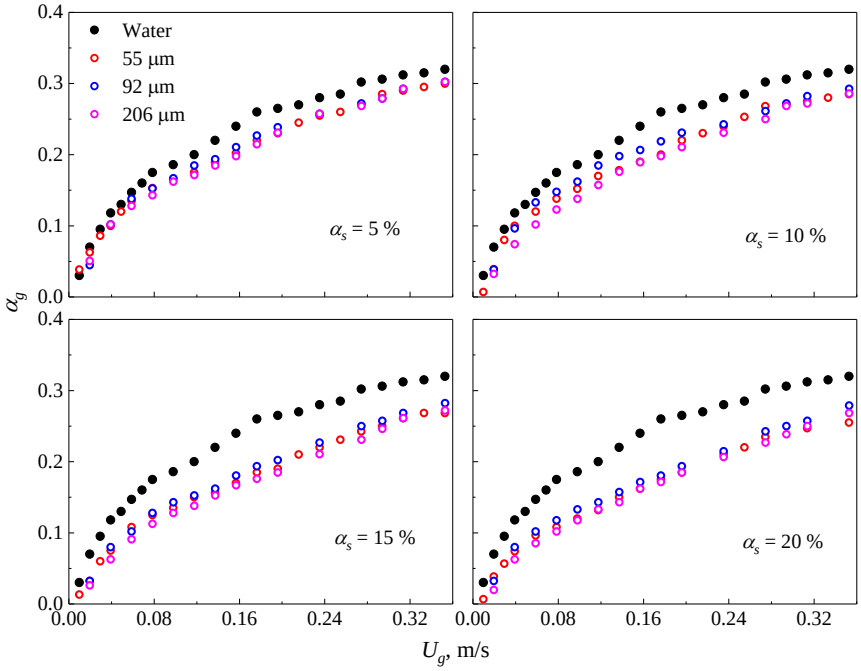

Figure 7. Effect of particle size on total gas holdup.

Volumetric mass transfer coefficients

Fig. 8 shows the effect of particle size on k_la in a wide range of α_s (0-20%). Overall, the particle size had only slight effect on k_la. Similar to gas holdup, k_la remained almost unchanged and then slightly decreased when increasing particle size from 55 to 206 μm. Compared with the literature, the effect of the presence of particles on the gas-liquid volumetric mass transfer coefficient was obtained in a much wider range of particle size and concentration in this work.

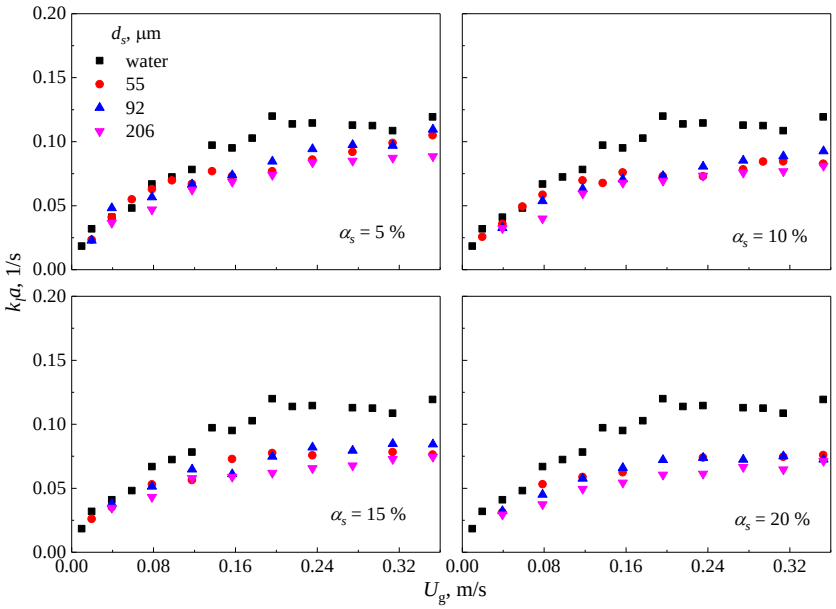

Figure 8. Effect of particle size on the volumetric mass transfer coefficients.

3. Empirical correlations and turbulence attenuation mechanism

3.1 Gas-liquid bubble column

3.1.1 Gas holdup

The calculation of gas holdup in a bubble column needs seven physical parameters, namely, superficial gas velocity U_g, gravitational acceleration g, bubble column size D_C, gas density ρ_g, liquid density ρ_l, liquid surface tension σ_l, and liquid viscosity μ_l:

$$\alpha_g = f\left(U_g, g, D_C, \rho_g, \rho_l, \sigma_l, \mu_l\right) \tag{5}$$

Since there are three basic dimensions, namely, mass (kg), length (m), and time (s), in the above seven parameters, according to the Buckingham's π theory, four dimensionless numbers are needed to determine the gas holdup:[5]

$$\pi_1 = \frac{U_g}{\sqrt{gD_C}},\ \pi_2 = \frac{gD_C^2\rho_l}{\sigma_l},\ \pi_3 = \frac{gD_C^3\rho_l^2}{\mu_l^2},\ \pi_4 = \frac{\rho_g}{\rho_l} \tag{6}$$

where π_1 is the Froude number Fr, π_2 is the Bond number Bo, π_3 is the Galilei number Ga, and π_4 is the density ratio r.

Therefore, the gas holdup in a gas-liquid bubble column was correlated as:

$$\alpha_g = c_1 \cdot \left(\frac{U_g}{\sqrt{gD_C}}\right)^{c_2} \cdot \left(\frac{gD_C^2\rho_l}{\sigma_l}\right)^{c_3} \cdot \left(\frac{gD_C^3\rho_l^2}{\mu_l^2}\right)^{c_4} \cdot \left(\frac{\rho_g}{\rho_l}\right)^{c_5} \tag{7}$$

By nonlinear regression to experimental data of α_g shown in Table 1 to determine the exponents, the final empirical correlation of the gas holdup in a gas-liquid bubble column is:

$$\alpha_g = 0.45\left(\frac{U_g}{\sqrt{gD_C}}\right)^{0.69} \cdot \left(\frac{gD_C^2\rho_l}{\sigma_l}\right)^{0.19} \cdot \left(\frac{gD_C^3\rho_l^2}{\mu_l^2}\right)^{0.03} \cdot \left(\frac{\rho_g}{\rho_l}\right)^{0.23} \tag{8}$$

($0.01 \le U_g \le 0.35$ m/s, $1.23 \le \rho_g \le 43.05$ kg/m^3, $714 \le \rho_l \le 1294$ kg/m^3, $24.6 \le \sigma_l \le 75.3$ mN/m, and $0.47 \le \mu_l \le 185$ mPa·s)

This is the same as that reported by Lakhdissi et al.[5], which is not surprising because the experimental data used in the regression were almost the same.

Table 1. Liquid properties and bubble column size data from the literature used in this work.

Ref.	Liquid	U_g, m/s	ρ_l, kg/m^3	μ_l, mPa·s	σ, mN/m	D_l,10^{-9} m^2/s	P, MPa	Data	D_C, m	H, m
Hashemi et al.[37]	Water	0.02-0.15	1000	1.0	72.5	2.0	0.1-2.5	k_la	0.10	1.2
Esmaeili et al.[38]	Water	0.01-0.32	1000	1.0	72.5		0.1-1.0	a_g	0.15	4.8
	Glucose	0.01-0.35	1294	185.0	74.3		0.1, 1.0	a_g		
	Boger	0.01-0.35	1251	135.0	75.3		0.1, 1.0	a_g		
Jordan et al.[39]	1-Butanol	0.01-0.21	809	2.9	24.6	1.38	0.1-1.0	k_la	0.10	2.4
Lin et al.[40]	Paratherm NF (300 K)	0.05-0.26	869	31.7	29.5		0.1, 3.5	a_g	0.05	0.8
	Paratherm NF (320 K)	0.04-0.26	859	10.7	28.0		0.1, 3.5	a_g		
	Paratherm NF (351 K)	0.04-0.29	847	4.7	26.0		0.1, 3.5	a_g		
Xing et al.[35]	Water	0.02-0.30	1000	1.0	72.5		0.1	a_g	0.19	2.5
	Glycerol solution (54.9 wt%)	0.01-0.28	1124	7.9	63.6		0.1	a_g		
	Glycerol solution (69.9 wt%)	0.01-0.28	1140	20.1	63.2		0.1	a_g		
	Glycerol solution (76.6 wt%)	0.01-0.27	1184	39.6	62.0		0.1	a_g		
Grund et al.[41]	Water	0.03-0.20	999	1.0	72.7		0.1	a_g, a	0.15	4.3
	Toluene	0.01-0.17	865	0.6	28.3		0.1	a_g		
	Ligroin	0.01-0.18	714	0.47	20.4		0.1	a_g		
Han et al.[36]	Water	0.01-0.45	1000	1.0	72.5	2.0	0.1-1.0	k_la	0.16	1.8
Lakhdissi et al.[5]	Water	0.004-0.26	1000	1.0	72.5	2.0	0.1	a_g, k_la	0.29	2.6
Terasaka et al.[42]	Water	0.01-0.14	1000	1.0	72.5	2.0	0.1	k_la	0.11	
Li et al.[20]	Water	0.05-0.35	1000	1.0	72.5		0.1	a_g	0.28	2.4
Gandhi et al.[43]	Water	0.05-0.26	1000	1.0	72.5		0.1	a_g	0.15	2.5
This work	Water	0.01-0.35	1000	1.0	72.5	2.0	0.1	a_g, k_la	0.19	2.5

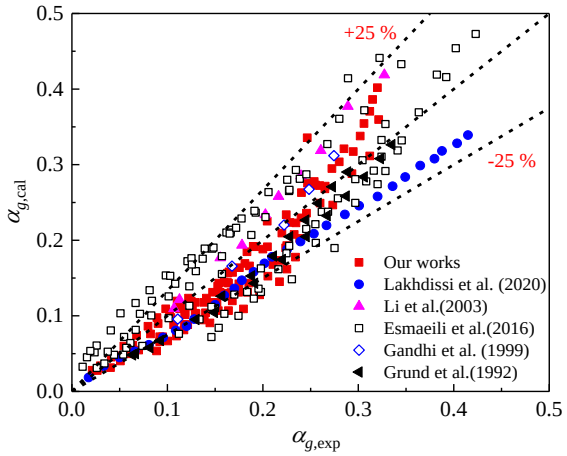

Figure 9. Parity plot for gas holdup in a gas-liquid bubble column with different liquids and operating parameters.

The comparison of the calculated gas holdup by Eq. (8) and experimental data is shown in Fig. 9. Considering that the experimental data were from different research groups and covered a wide range of operating conditions, the agreement between the correlation and experimental data is satisfactory.

3.1.2 Volumetric mass transfer coefficient

The calculation of k_la needs one more physical parameter, namely, the diffusion coefficient D_l:

$$k_l a = f\left(U_g, g, D_C, \rho_g, \rho_l, \sigma_l, \mu_l, D_l\right) \tag{9}$$

Therefore, one more dimensionless number, namely, the Schmidt number Sc, was added:[44]

$$\pi_5 = \mathrm{Sc} = \frac{\mu_l}{\rho_l D_l} \tag{10}$$

By nonlinear regression based on the collected experimental data of k_la shown in Table 1, the volumetric mass transfer coefficient for a gas-liquid bubble column was

correlated as:

$$\frac{k_l a D_C^2}{D_l} = 0.4 \cdot \left(\frac{U_g}{\sqrt{g D_C}} \right)^{0.76} \cdot \left(\frac{g D_C^2 \rho_l}{\sigma_l} \right)^{0.83} \cdot \left(\frac{g D_C^3 \rho_l^2}{\mu_l^2} \right)^{0.34} \cdot \left(\frac{\rho_g}{\rho_l} \right)^{0.25} \cdot \left(\frac{\mu_l}{\rho_l D_l} \right)^{0.5} \quad (11)$$

($0.01 \le U_g \le 0.45$ m/s, $1.23 \le \rho_g \le 30.75$ kg/m^3, $809 \le \rho_l \le 1000$ kg/m^3, $24.6 \le \sigma_l \le 72.5$ mN/m, $1 \le \mu_l \le 2.9$ mPa·s and $1.38\times10^{-9} \le D_l \le 2.0\times10^{-9}$ m^2/s)

Table 2. Empirical correlations for $k_l a$ in the literature.

Author	Correlations
Akita and Yoshida[45]	$\frac{k_l a D_C^2}{D_l} = 0.6 \left(\frac{\mu_l}{\rho_l D_l} \right)^{0.5} \left(\frac{g D_C^2 \rho_l}{\sigma_l} \right)^{0.62} \left(\frac{g D_C^3 \rho_l^2}{\mu_l^2} \right)^{0.31} \varepsilon_g^{1.1}$
Nakanoh and Yoshida[46]	$\frac{k_l a D_C^2}{D_l} = 0.09 \left(\frac{\mu_l}{\rho_l D_l} \right)^{0.5} \left(\frac{g D_C^2 \rho_l}{\sigma_l} \right)^{0.75} \left(\frac{g D_C^3 \rho_l^2}{\mu_l^2} \right)^{0.39} \left(\frac{U_g}{\sqrt{g D_C}} \right)$
Öztürk et al.[44]	$\frac{k_l a d_b^2}{D_l} = 0.62 \left(\frac{\mu_l}{\rho_l D_l} \right)^{0.5} \left(\frac{g \rho_l d_b^2}{\sigma} \right)^{0.33} \left(\frac{g \rho_l^2 d_b^3}{\mu_l^2} \right)^{0.29} \left(\frac{U_g}{\sqrt{g d_b}} \right)^{0.68} \left(\frac{\rho_g}{\rho_l} \right)^{0.04}$, $d_b = 0.003$ m

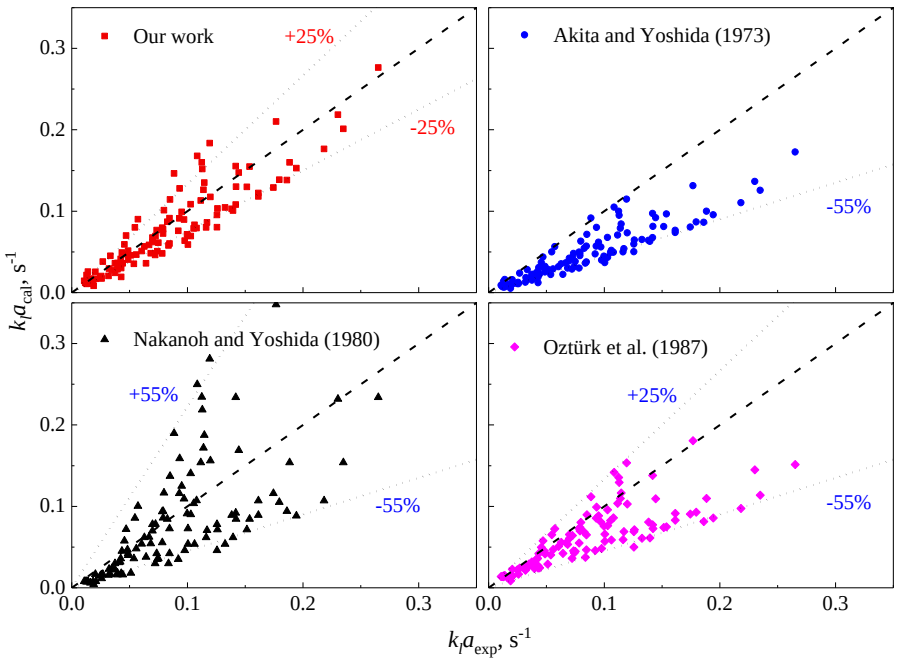

Figure 10. Parity plots for $k_l a$ in a gas-liquid bubble column due to different correlations.

The three empirical correlations for $k_l a$ in the literature[44-46] listed in Table 2, were

compared with the correlation developed in this work. As shown in Fig. 10, our correlation proposed is more accurate, due to that it uses regression to the experimental data which cover a wider range of operating conditions.

3.2 Slurry bubble column

Many researchers use a two-phase model for calculating three-phase hydrodynamics by combining the liquid and solid phases into a pseudo-homogeneous phase. In this section, we discuss the accuracy of the two-phase approach with corrected slurry properties for calculating gas holdup and k_la in a slurry bubble column.

After including a correction factor for the slurry density and viscosity, Eqs. (8) and (11) are modified as:

$$\alpha_{g,sl*} = 0.45\left(\frac{U_g}{\sqrt{gD_C}}\right)^{0.69}\cdot\left(\frac{gD_C^2\rho_{sl}}{\sigma_l}\right)^{0.19}\cdot\left(\frac{gD_C^3\rho_{sl}^2}{\mu_{sl}^2}\right)^{0.03}\cdot\left(\frac{\rho_g}{\rho_{sl}}\right)^{0.23} \quad (13)$$

$$\frac{k_{sl*}aD_C^2}{D_{sl}} = 0.4\cdot\left(\frac{U_g}{\sqrt{gD_C}}\right)^{0.76}\cdot\left(\frac{gD_C^2\rho_{sl}}{\sigma_l}\right)^{0.83}\cdot\left(\frac{gD_C^3\rho_{sl}^2}{\mu_{sl}^2}\right)^{0.34}\cdot\left(\frac{\rho_g}{\rho_{sl}}\right)^{0.25}\cdot\left(\frac{\mu_{sl}}{\rho_{sl}D_{sl}}\right)^{0.5} \quad (14)$$

The slurry density was calculated using the ideal volume mixing method $\rho_{sl} = \alpha_s\rho_s + (1-\alpha_s)\rho_l$, and the slurry viscosity was calculated using the correlation $\mu_{sl} = (1-\alpha_s)^{-2.5}$ for $\alpha_s \le 5\%$ and $\mu_{sl} = (1-1.35\alpha_s)^{-2.5}$ for $\alpha_s > 5\%$ proposed by Roscoe[22]. The effect of solid particle on the liquid surface tension was neglected. The diffusion coefficient, D_{sl}, was calculated by the empirical correlation $D_{sl} = D_l\cdot(\mu_{sl}/\mu_l)^{-0.57}$ proposed by Öztürk et al.[44].

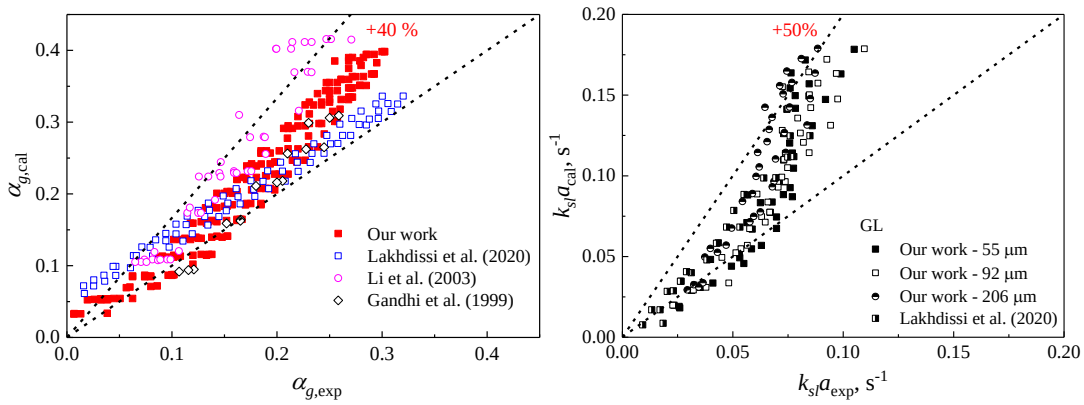

Figure 11. Parity plot for gas holdups (left) and k_la (right) of slurry bubble column using the empirical correlations of gas-quasi-homogeneous liquid system.

Fig. 11 shows the comparison of calculated gas holdup by Eq. (13) and calculated k_la by Eq. (14) with experimental data. Calculated gas holdup and k_la by the two-phase approach were both higher than experimental data, that is, the pseudo two-phase approach could not accurately calculate the hydrodynamics and mass transfer rate in a three-phase slurry bubble column.

3.3 Parameter for liquid turbulence attenuation

An et al.[28] studied the effect of particle concentration on slurry viscosity, bubble coalescence, gas-liquid drag force, and liquid turbulence, and found that the effect of turbulence attenuation dominated the hydrodynamics of a slurry bubble column. However, the mechanism of liquid turbulence attenuation was left unknown, and the effect of particle size could not be calculated.

In this work, a model of liquid turbulence attenuation by particles was developed by equating the energy consumed by the motion of particles to the attenuated liquid turbulence energy calculated from the turbulent energy spectrum. The following

assumptions are made:

(1) Only the most important drag force is considered in the movement of the particles;

(2) The work time per unit fluid in driving the particles to move equal to the lifetime of the liquid phase turbulent eddy;

(3) When calculating the slip velocity between particles and fluid, the interaction of bubbles and particles is ignored, but bubble-induced turbulence in the liquid phase is included;

(4) When calculating the energy of turbulent eddies, only the energy in the inertial energy spectrum is included, which conforms to the Kolmogorov inertial energy spectrum shown in Fig. 12.

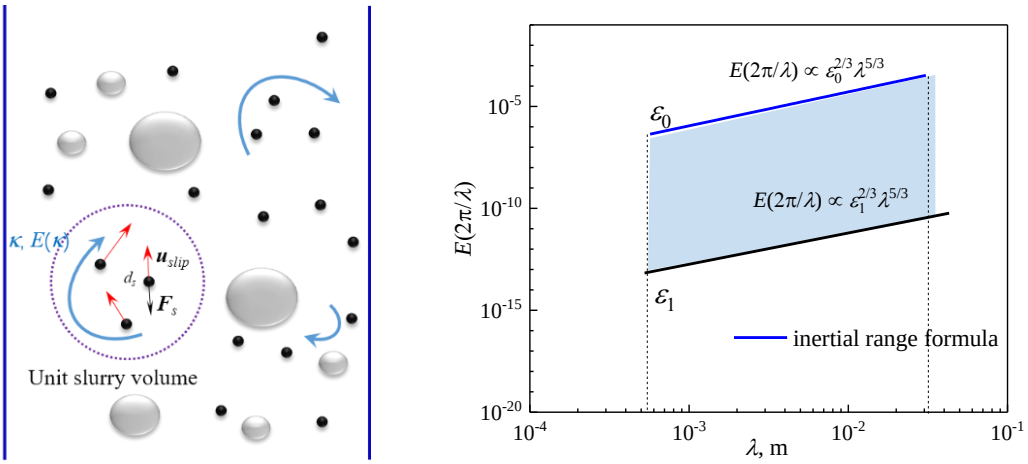

Figure 12. Schematic of liquid turbulence attenuation by the particle effect (left) and turbulent spectrum (right).

The energy per unit slurry volume dissipated by the relative motion of particles, E_p, was estimated by:[30,47]

$$E_p = n_s F_s u_{slip} \tau_e \tag{15}$$

$$F_s = \frac{1}{2} C_{Ds} \rho_l u_{slip}^2 A_{ps} \tag{16}$$

$$\tau_e = \left(\varepsilon_1 / L^2\right)^{-1/3},\ L = k_1^{3/2} / \varepsilon_1 \tag{17}$$

$$C_{Ds} = \begin{cases} \dfrac{24}{\mathrm{Re}_s}\left(1 + 0.15\mathrm{Re}_s^{0.687}\right) & \mathrm{Re}_s \le 1000 \\ 0.44 & \mathrm{Re}_s > 1000 \end{cases} \tag{18}$$

where $n_s = 6\alpha_s/\pi d_s^3$ is the number of particles per unit volume of slurry, F_s is the drag force on the particles, C_{Ds} is the drag coefficient of the particle, d_s is the particle diameter, Re_s is the particle Reynolds number, $A_{ps} = \pi d_s^2/4$ is the cross sectional area of a particle, τ_e is the turbulent eddy life time, ε_1 and k_1 are the turbulent dissipation rate and turbulent kinetic energy, respectively, and L is an integral scale.

The particle slip velocity u_{slip} is calculated from the experimental results of Palani et al.[48]:

$$u_{slip} = 0.9 u_l \left(\frac{\rho_s - \rho_l}{\rho_l}\right)^{0.0167} \left(\frac{d_s}{d_0}\right),\ d_0 = 550\ \mu\mathrm{m} \tag{19}$$

$$u_l = \sqrt{2}\left(\varepsilon_1 L\right)^{1/3} \tag{20}$$

The calculations of ε_0 and k_0 used the equations in Wang et al. [49]:

$$\varepsilon_0 = C_\mu^{3/4}\left[0.04\left(U_g/a_g\right)^2\right]^{3/2} / \left(0.07 D_c\right) + \alpha_g g U_g \tag{21}$$

$$k_0 = 0.04\left(U_g/a_g\right)^2 + 0.25\alpha_g g U_g^2 \tag{22}$$

where ε_0 and k_0 were the initial turbulent dissipation rate and turbulent kinetic energy of the pure liquid phase with considering bubble-induced turbulence, respectively.

Using the turbulent energy spectrum,[50] the attenuated energy per unit volume of slurry can be calculated by:

$$E_p = \Omega(\varepsilon_0) - \Omega(\varepsilon_1) \tag{23}$$

$$\Omega(\varepsilon) = -\int_{\frac{2\pi}{11.4\eta}}^{\frac{2\pi}{L}} \rho_{sl} E_\kappa d\kappa = 3\left[\left(\frac{2\pi}{L}\right)^{-2/3} - \left(\frac{2\pi}{11.4\eta}\right)^{-2/3}\right]\rho_{sl}\varepsilon^{2/3} \tag{24}$$

where ε_0 is the initial liquid turbulent dissipation rate, and ε_1 is the liquid turbulent dissipation rate after liquid attenuation. Ω is the turbulence energy, E_κ is the turbulence spectrum, $= 2\varepsilon^{2/3}\kappa^{-5/3}$, κ is the wave number, and η is the Kolmogorov scale, $= (\mu_{sl}/\rho_{sl})^{3/4}\varepsilon^{-1/4}$.

By combining Eqs. (15) and (23), the liquid turbulent dissipation rate ε_1 after liquid attenuation by the solid particles can be calculated as:

$$\varepsilon_1 = \left\{\varepsilon_0^{2/3} - \frac{E_p}{3\left[\left(\frac{2\pi}{L}\right)^{-2/3} - \left(\frac{2\pi}{11.4\eta}\right)^{-2/3}\right]\rho_l}\right\}^{3/2} \tag{25}$$

Based on above derivation, the following correlation parameter ψ_s was proposed for liquid turbulence attenuation:

$$\psi_s = \frac{\varepsilon_1}{\varepsilon_0} = \left\{1 - \frac{2^{-4/3}\pi^{2/3}\alpha_s C_{Ds} u_{slip}^3 L^{2/3}}{d_s\left[L^{2/3} - (11.4\eta)^{2/3}\right]\varepsilon_0}\right\}^{3/2} \tag{26}$$

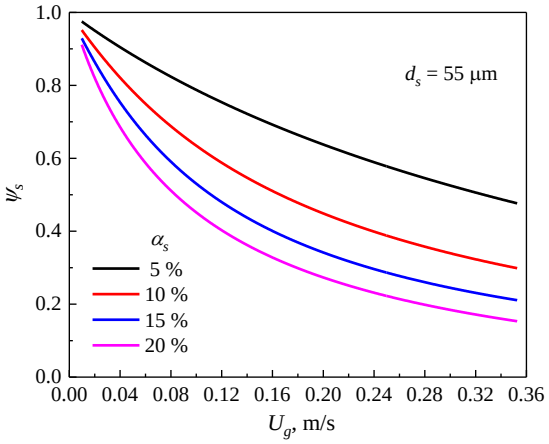

Figure 13. Effect of particle concentration on the liquid turbulence attenuation parameter (ψ_s) at different superficial gas velocities.

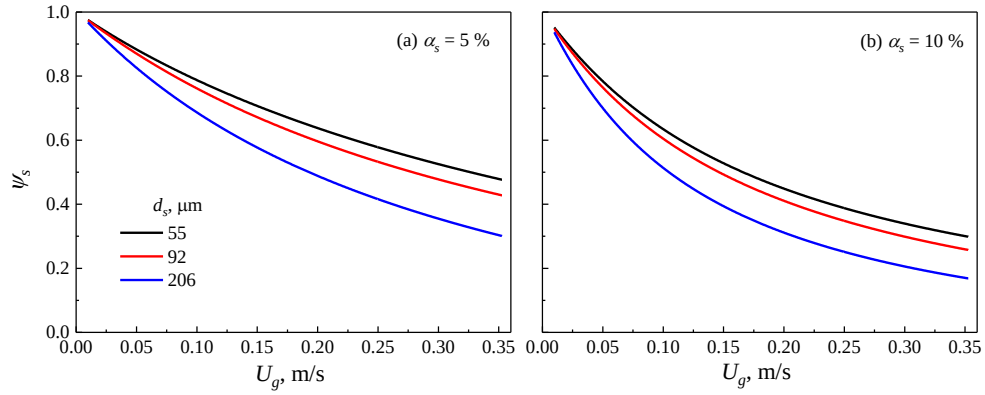

Figure 14. Effect of particle size on the liquid turbulence attenuation parameter (ψ_s).

Fig. 13 shows the effect of particle concentration on the liquid turbulence attenuation parameter, which shows that with increasing α_s, it significantly decreased. The effect of particle size on this parameter ψ_s is shown in Fig. 14, which shows that with increasing particle size from 55 to 92 μm, liquid turbulence attenuation increased slightly, then it significantly increased with an increase in particle size to 206 μm.

3.4 Gas-liquid-solid three-phase slurry bubble column

We found that the effect of particle concentration and particle size on liquid turbulence attenuation as calculated in Section 3.3 was the same trend as the effect of α_s and d_s on the hydrodynamics and mass transport in a slurry bubble column described in Section 2.3. Therefore, we combined the empirical pseudo two-phase correlations for a slurry bubble column with the liquid turbulence attenuation parameter correlation, to get a new semi-empirical correlation for gas holdup and k_la in a three-phase slurry bubble column.

By combining Eqs. (13) and (14) with Eq. (26), the following semi-empirical correlations for gas holdup and k_la in a three-phase slurry bubble column were obtained:

$$\alpha_{g,gls} = 0.45\left(\frac{U_g}{\sqrt{gD_C}}\right)^{0.69}\cdot\left(\frac{gD_C^2\rho_{sl}}{\sigma_l}\right)^{0.19}\cdot\left(\frac{gD_C^3\rho_{sl}^2}{\mu_{sl}^2}\right)^{0.03}\cdot\left(\frac{\rho_g}{\rho_{sl}}\right)^{0.23}\cdot\psi_s^{0.062} \quad (27)$$

$$\frac{k_{sl}aD_C^2}{D_{sl}} = 0.4\cdot\left(\frac{U_g}{\sqrt{gD_C}}\right)^{0.76}\cdot\left(\frac{gD_C^2\rho_l}{\sigma_l}\right)^{0.83}\cdot\left(\frac{gD_C^3\rho_{sl}^2}{\mu_{sl}^2}\right)^{0.34}\cdot\left(\frac{\rho_g}{\rho_{sl}}\right)^{0.25}\cdot\left(\frac{\mu_{sl}}{\rho_{sl}D_{sl}}\right)^{0.5}\cdot\psi_s^{0.1} \quad (28)$$

where the exponent values of 0.062 and 0.1 for ψ_s were obtained by regression using our experimental data listed in Table 3.

Table 3. Experimental details of slurry bubble columns used in the literature and this work.

Source	Particle size, μm	Volume fraction α_s	H, m	D_C, m
Lakhdissi et al.[5]	35, 71 and 156	0 – 5%	2.6	0.29
Li et al. [20 20]	11, 35 and 93	0 – 20%	2.4	0.28
Gandhi et al.[43]	35	0 – 20%	2.5	0.15
This work	55, 92 and 206	0	2.5	0.19

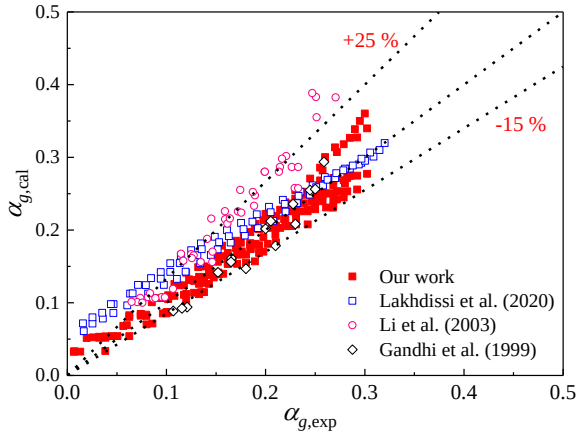

Figure 15. Parity plot for gas holdups in a slurry bubble column calculated by our correlation that includes liquid turbulence attenuation.

The comparison of calculated gas holdup by Eq. (27) and k_la by Eq. (28) with experimental data was shown in Fig. 15 and Fig. 16, respectively. Gas holdup and k_la both agreed satisfactorily with the experimental data, which showed that after including liquid turbulence attenuation, the modified two-phase empirical correlations could

accurately calculated the hydrodynamics and mass transfer coefficients in a three-phase slurry bubble column.

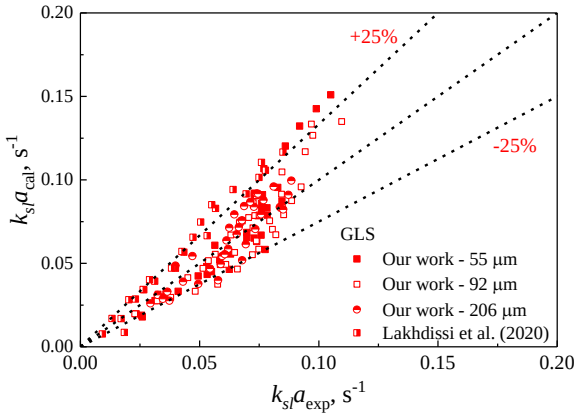

Figure 16. Parity plot for k_la in a slurry bubble column from our correlation that includes liquid turbulence attenuation.

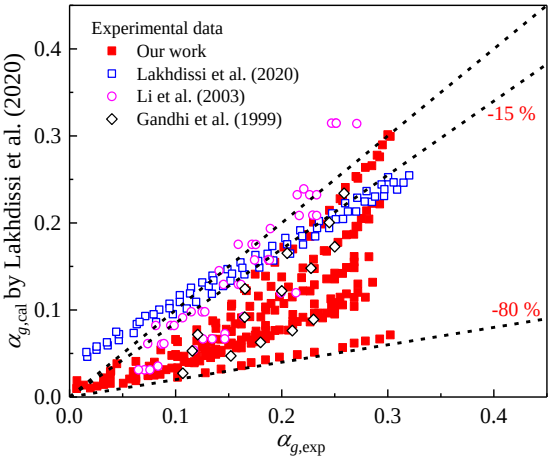

Figure 17. Parity plot for gas holdups of slurry bubble column by the correction of Lakhdissi et al. (2020).

To compare the latest model by Lakhdissi et al.[5] with our model, calculated gas holdup using the correlation of Lakhdissi et al.[5] (listed in Table 4) are compared with the same experimental data. This is shown in Fig. 17. The correlation by Lakhdissi et al.[5] gave values that were much lower than the experimental data from our work and

from Gandhi et al.[43] In contrast, our proposed correction could accurately reproduce whole set of experimental data, which is due to that the dominant effect of liquid turbulence attenuation was taken into account.

Table 4. Empirical correlation for gas holdup of slurry bubble column by Lakhdissi et al.[5]

Items	Equation
Gas holdup	$\alpha_{g,Lakhdissi} = \alpha_{g,sl*} \cdot \left[\left(1 - E_C\right) \cdot \left(1 - \alpha_s\right) \right]^{5.43}$
Collision efficiency	$E_C = E_{C-SU} \sin^2 \theta_t \cdot e^{\left\{ 3K_3 \left[\cos\theta_t \left(\ln \frac{3}{E_{C-SU}} - 1.8 \right) - \frac{2+\cos^3\theta_t - 3\cos\theta_t}{2E_{C-SU}\sin^2\theta_t} \right] \right\}}$
Sutherland model collision efficiency	$E_{C-SU} = \frac{3d_s}{d_b}$
The angle of tangency	$\theta_t = \arcsin\left\{ 2\beta \left[\left(1+\beta^2\right)^{1/2} - \beta \right] \right\}^{1/2}$
Model parameter	$\beta = \frac{4E_{C-SU}}{9K_3}, K_3 = \mathrm{St}\frac{\rho_s - \rho_{sl}}{\rho_s}, \mathrm{St} = \frac{V_b \rho_s d_s^2}{9\mu_{sl} d_b}$
Bubble rise velocity correlation	$V_b = \sqrt{gD_C} \cdot 0.21 \cdot \mathrm{Fr}^{0.51} \cdot \mathrm{Bo}^{-0.96} \cdot \mathrm{Ga}^{-0.01} \cdot \left(\rho_g/\rho_{sl}\right)^{-1.6}$
Bubble size correlation	$d_b = D_C \cdot 0.6 \cdot \mathrm{Fr}^{0.53} \cdot \mathrm{Bo}^{0.35} \cdot \mathrm{Ga}^{-0.14} \cdot \left(\rho_g/\rho_{sl}\right)^{0.17}$

4. Conclusions

The effects of particle concentration and particle size on hydrodynamics and mass transport in a slurry bubble column were experimentally studied. With increasing particle concentration, the averaged gas holdup, gas holdup of small bubbles and gas-liquid volumetric mass transfer coefficient significantly decreased, while the gas holdup of large bubbles increased slightly. When the particle size was increased from 55 to 92 μm, the averaged gas holdup and $k_l a$ remained unchanged, but they decreased significantly with a further increase of particle size to 206 μm. A semi-empirical model of liquid turbulence attenuation was developed in order to include liquid turbulence

attenuation into the effects of particle concentration and size. This gave a parameter whose value was obtained by regression with extensive experimental data from gas-liquid bubble column and gas-liquid-solid slurry bubble column in a wide operating conditions and liquid properties. This parameter ψ_s was included in the following semi-empirical correlations and it enabled then to accurately calculate the gas holdup α_g and volumetric mass transfer coefficient k_la:

For a gas-liquid bubble column:

$$\alpha_g = 0.45\left(\frac{U_g}{\sqrt{gD_C}}\right)^{0.69}\cdot\left(\frac{gD_C^2\rho_l}{\sigma_l}\right)^{0.19}\cdot\left(\frac{gD_C^3\rho_l^2}{\mu_l^2}\right)^{0.03}\cdot\left(\frac{\rho_g}{\rho_l}\right)^{0.23}$$

$$\frac{k_l a D_C^2}{D_l} = 0.4\cdot\left(\frac{U_g}{\sqrt{gD_C}}\right)^{0.76}\cdot\left(\frac{gD_C^2\rho_l}{\sigma_l}\right)^{0.83}\cdot\left(\frac{gD_C^3\rho_l^2}{\mu_l^2}\right)^{0.34}\cdot\left(\frac{\rho_g}{\rho_l}\right)^{0.25}\cdot\left(\frac{\mu_l}{\rho_l D_l}\right)^{0.5}$$

For a gas-liquid-solid three-phase bubble column:

$$\alpha_{g,gls} = 0.45\left(\frac{U_g}{\sqrt{gD_C}}\right)^{0.69}\cdot\left(\frac{gD_C^2\rho_{sl}}{\sigma_{sl}}\right)^{0.19}\cdot\left(\frac{gD_C^3\rho_{sl}^2}{\mu_{sl}^2}\right)^{0.03}\cdot\left(\frac{\rho_g}{\rho_{sl}}\right)^{0.23}\cdot\psi_s^{0.062}$$

$$\frac{k_{sl} a D_C^2}{D_{sl}} = 0.4\cdot\left(\frac{U_g}{\sqrt{gD_C}}\right)^{0.76}\cdot\left(\frac{gD_C^2\rho_{sl}}{\sigma_{sl}}\right)^{0.83}\cdot\left(\frac{gD_C^3\rho_{sl}^2}{\mu_{sl}^2}\right)^{0.34}\cdot\left(\frac{\rho_g}{\rho_{sl}}\right)^{0.25}\cdot\left(\frac{\mu_{sl}}{\rho_{sl} D_{sl}}\right)^{0.5}\cdot\psi_s^{0.1}$$

Acknowledgments

The authors thank the financial supports by the National Key Research and Development Program of China (No. 2018YFB0604804).

Notations

$C_{O_2}(t)$	dissolved oxygen concentration, ppm
D_c	Column diameter, m
D_l	diffusion coefficient, $m^2 \cdot s^{-1}$
d_b	bubble size, m

d_s	particle size, μm
u_{slip}	particle slip velocity, $m \cdot s^{-1}$
U_g	superficial gas velocity, $m \cdot s^{-1}$
k_la	gas-liquid volumetric mass transfer coefficient

Greek letters

α_g	gas holdup, dimensionless
ε	turbulent energy dissipation rate, $m^2 \cdot s^{-3}$
α_s	volume fraction of particles, dimensionless
ρ_{sl}	slurry density, $kg \cdot m^{-3}$
ρ_l	liquid density, $kg \cdot m^{-3}$
ρ_s	particle density, $kg \cdot m^{-3}$
σ_l	liquid surface tension, $N \cdot m^{-1}$
ψ_s	Correlation parameter for considering liquid turbulence attenuation, dimensionless

References

1. Wang TF, Wang JF, Jin Y. Slurry reactors for gas-to-liquid processes: A review. *Ind. Eng. Chem. Res.* 2007;46(18):5824-5847.

2. Basha OM, Sehabiague L, Abdel-Wahab A, Morsi BI. Fischer-Tropsch synthesis in slurry bubble column reactors: Experimental investigations and modeling - A review. *Int. J. Chem. React. Eng.* 2015;13(3):201-288.

3. Kulkarni AA, Joshi JB. Bubble formation and bubble rise velocity in gas-liquid systems: A review. *Ind. Eng. Chem. Res.* 2005;44(16):5873-5931.

4. Shu SL, Vidal D, Bertrand F, Chaouki J. Multiscale multiphase phenomena in bubble column reactors: A review. *Renew Energ.* 2019;141:613-631.

5. Lakhdissi EM, Soleimani I, Guy C, Chaouki J. Simultaneous effect of particle size and solid concentration on the hydrodynamics of slurry bubble column reactors. *AIChE J.* 2020;66(2).

6. Zhou X, Ma Y, Liu M, Zhang Y. CFD-PBM simulations on hydrodynamics and

gas-liquid mass transfer in a gas-liquid-solid circulating fluidized bed. *Powder Technol.* 2020;362:57-74.

7. Zhou R, Yang N, Li J. A conceptual model for analyzing particle effects on gas-liquid flows in slurry bubble columns. *Powder Technol.* 2020;365:28-38.

8. Lakhdissi EM, Fallahi A, Guy C, Chaouki J. Effect of solid particles on the volumetric gas liquid mass transfer coefficient in slurry bubble column reactors. *Chem. Eng. Sci.* 2020;227:115912.

9. Tyagi P, Buwa VV. Dense gas-liquid-solid flow in a slurry bubble column: Measurements of dynamic characteristics, gas volume fraction and bubble size distribution. *Chem. Eng. Sci.* 2017;173:346-362.

10. Rabha S, Schubert M, Hampel U. Intrinsic flow behavior in a slurry bubble column: A study on the effect of particle size. *Chem. Eng. Sci.* 2013;93:401-411.

11. Rabha S, Schubert M, Wagner M, Lucas D, Hampel U. Bubble size and radial gas hold-up distributions in a slurry bubble column using ultrafast electron beam X-Ray tomography. *AIChE J.* 2013;59(5):1709-1722.

12. Jin H, Yang S, He G, Liu D, Tong Z, Zhu J. Gas–liquid mass transfer characteristics in a gas–liquid–solid bubble column under elevated pressure and temperature. *Chinese J. Chem. Eng.* 2014;22(9):955-961.

13. Behkish A, Lemoine R, Sehabiague L, Oukaci R, Morsi BI. Gas holdup and bubble size behavior in a large-scale slurry bubble column reactor operating with an organic liquid under elevated pressures and temperatures. *Chem. Eng. J.* 2007;128(2):69-84.

14. Li H, Prakash A. Influence of slurry concentrations on bubble population and their rise velocities in a three-phase slurry bubble column. *Powder Technol.* 2000;113(1):158-167.

15. Vandu CO, Koop K, Krishna R. Volumetric mass transfer coefficient in a slurry bubble column operating in the heterogeneous flow regime. *Chem. Eng. Sci.* 2004;59(22-23):5417-5423.

16. Sehabiague L, Morsi BI. Hydrodynamic and mass transfer characteristics in a

large-scale slurry bubble column reactor for gas mixtures in actual Fischer-Tropsch cuts. *Int. J. Chem. React. Eng.* 2013;11.

17. Mena P, Ferreira A, Teixeira JA, Rocha F. Effect of some solid properties on gas-liquid mass transfer in a bubble column. *Chem. Eng. Process.* 2011;50(2):181-188.

18. Ojima S, Hayashi K, Tomiyama A. Effects of hydrophilic particles on bubbly flow in slurry bubble column. *Int. J. Multiphase Flow.* 2014;58:154-167.

19. Ojima S, Sasaki S, Hayashi K, Tomiyama A. Effects of particle diameter on bubble coalescence in a slurry bubble column. *J. Chem. Eng. Jpn.* 2015;48(3):181-189.

20. Li H, Prakash A, Margaritis A, Bergougnou MA. Effects of micron-sized particles on hydrodynamics and local heat transfer in a slurry bubble column. *Powder Technol.* 2003;133(1-3):171-184.

21. Einstein A. Effect of suspended rigid spheres on viscosity. *Ann. Phys.* 1906;19:289–306.

22. Roscoe R. The viscosity of suspensions of rigid spheres. *Br. J. Appl. Phys.* 1952;3(8):267.

23. Toda K, Furuse H. Extension of Einstein's viscosity equation to that for concentrated dispersions of solutes and particles. *J. Biosci. Bioeng.* 2006;102(6):524-528.

24. Sato Y, Sekoguchi K. Liquid velocity disteribution in two-phase bubble flow. *Int. J. Muhiphase Flow.* 1975;2(1):79-95.

25. Happel J. Viscosity of suspensions of uniform spheres. *J. Appl. Phys.* 1957;28(11):1288-1292.

26. Su W, Shi X, Wu Y, Gao J, Lan X. Simulation on the effect of particle on flow hydrodynamics in a slurry bed. *Powder Technol.* 2020;361:1006-1020.

27. Wang P, Cilliers JJ, Neethling SJ, Brito-Parada PR. The behavior of rising bubbles covered by particles. *Chem. Eng. J.* 2019;365:111-120.

28. An M, Guan XP, Yang N. Modeling the effects of solid particles in CFD-PBM simulation of slurry bubble columns. *Chem. Eng. Sci.* 2020;223:115743.

29. Squires KD, Eaton JK. Effect of selective modification of turbulence on two-equation models for particle-laden turbulent flows. *J. Fluid. Eng.* 1994;116(4):778-784.

30. Schneiders L, Fröhlich K, Meinke M, Schröder W. The decay of isotropic turbulence carrying non-spherical finite-size particles. *J. Fluid Mech.* 2019;875:520-542.

31. Li W, Zhong W. CFD simulation of hydrodynamics of gas–liquid–solid three-phase bubble column. *Powder Technol.* 2015;286:766-788.

32. An M, Guan XP, Yang N, Bu Y, Xu M, Men Z. Effects of internals on fluid dynamics and reactions in pilot-scale slurry bubble column reactors: A CFD study for Fischer-Tropsch synthesis. *Chem. Eng. Process.* 2018;132:194-207.

33. Troshko AA, Zdravistch F. CFD modeling of slurry bubble column reactors for Fisher–Tropsch synthesis. *Chem. Eng. Sci.* 2009;64(5):892-903.

34. Mamabolo BA, Nkazi D. Modeling of a slurry bubble column reactor using a two-phase two-bubble class approach-A hydrodynamics study. *Energ. Fuel.* 2019;33(1):612-628.

35. Xing CT, Wang TF, Wang JF. Experimental study and numerical simulation with a coupled CFD–PBM model of the effect of liquid viscosity in a bubble column. *Chem. Eng. Sci.* 2013;95:313-322.

36. Han L, Al-Dahhan MH. Gas–liquid mass transfer in a high pressure bubble column reactor with different sparger designs. *Chem. Eng. Sci.* 2007;62(1):131-139.

37. Hashemi S, Macchi A, Servio P. Gas–liquid mass transfer in a slurry bubble column operated at gas hydrate forming conditions. *Chem. Eng. Sci.* 2009;64(16):3709-3716.

38. Esmaeili A, Farag S, Guy C, Chaouki J. Effect of elevated pressure on the hydrodynamic aspects of a pilot-scale bubble column reactor operating with non-Newtonian liquids. *Chem. Eng. J.* 2016;288:377-389.

39. Jordan U, Schumpe A. The gas density effect on mass transfer in bubble columns with organic liquids. *Chem. Eng. Sci.* 2001;56(21-22):6267-6272.

40. Lin TJ, Tsuchiya K, Fan LS. Bubble flow characteristics in bubble columns at

elevated pressure and temperature. *AIChE J.* 1998;44(3):545-560.

41. Grund G, Schumpe A, Deckwer WD. Gas-liquid mass-transfer in a bubble column with organic liquids. *Chem. Eng. Sci.* 1992;47(13-14):3509-3516.

42. Terasaka K, Hullmann D, Schumpe A. Mass transfer in bubble columns studied with an oxygen optode. *Chem. Eng. Sci.* 1998;53(17):3181-3184.

43. Gandhi B, Prakash A, Bergougnou MA. Hydrodynamic behavior of slurry bubble column at high solids concentrations. *Powder Technol.* 1999;103(2):80-94.

44. Ozturk SS, Schumpe A, Deckwer WD. Organic liquids in a bubble column - holdups and mass-transfer coefficients. *AIChE J.* 1987;33(9):1473-1480.

45. Akita K, Yoshida F. Gas holdup and volumetric mass transfer coefficient in bubble columns. Effects of liquid properties. *Ind. Eng. Chem. Proc. Dd.* 1973;12(1):76-80.

46. Nakanoh M, Yoshida F. Gas absorption by Newtonian and Non-Newtonian liquids in a bubble column. *Ind. Eng. Chem. Proc. Dd.* 1980;19(1):190-195.

47. Schneiders L, Meinke M, Schröder W. Direct particle–fluid simulation of Kolmogorov-length-scale size particles in decaying isotropic turbulence. *J. Fluid Mech.* 2017;819:188-227.

48. Palani N, Ramalingam V, Ramadoss G, Seeniraj RV. Study of slip velocity and application of drift-flux model to slip velocity in a liquid–solid circulating fluidized bed. *Adv. Powder Technol.* 2011;22(1):77-85.

49. Wang TF, Wang JF, Jin Y. A CFD-PBM coupled model for gas-liquid flows. *AIChE J.* 2006;52(1):125-140.

50. Solsvik J, Jakobsen HA. A review of the statistical turbulence theory required extending the population balance closure models to the entire spectrum of turbulence. *AIChE J.* 2016;62(5):1795-1820.